GEOLOGIC EVIDENCE FOR LIMITED GROUND MOTION DAMAGE IN THE TOPOPAH SPRING TUFF, YUCCA MOUNTAIN, NEVADA

David Buesch
U.S. Geological Survey, Yucca Mountain Project Branch, Las Vegas, Nevada

Introduction

Geologic data from the Topopah Spring Tuff at Yucca Mountain, Nevada, have been compiled and re-examined in the context of how the lithostratigraphic features such as lithophysae (cavities in the tuff, Figure 1) and fractures were formed and whether these features show evidence of seismically induced shear or strain. This evaluation was conducted to better understand the type and amount of potential damage that might have occurred to the rocks at Yucca Mountain during the 12.8 million-year history since the Topopah Spring Tuff was deposited. The Topopah Spring Tuff is the focus of this study for seven main reasons. 1) The lower part of the tuff is the host to the proposed repository for high-level radioactive waste and spent nuclear fuel. 2) The densely welded and crystallized lithostratigraphic units in the Topopah Spring Tuff (Buesch and others, 1996) that include the repository horizon consist of the lower part of the upper lithophysal zone and the middle nonlithophysal and lower lithophysal zones, and the upper part of the lower nonlithophysal zone. 3) A lot of data on fractures and lithophysae have been collected from the tunnels, which are referred to as the Exploratory Studies Facility (ESF) and the Enhanced Characterization of the Repository Block (ECRB) cross drift, and from surface- and tunnel-based boreholes. 4) Studies of the Topopah Spring Tuff and other variously welded and crystallized pyroclastic flow deposits (or ignimbrites) resulted in development of a petrogenetic sequence (spatial and temporal relations) for features in these rocks for the time period between deposition and completion of the cooling phase of the deposit (Buesch and Spengler, 1998; Buesch and others, 1999). 5) Rock properties, including mechanical properties, have been measured in laboratories and rock mechanics models have been developed. 6) Results of rock mechanics modeling indicate various types of lithophysae-fracture relations and damage to the rock mass would occur in rocks that have mechanically "failed" and have experienced static or dynamic strains beyond values of 0.1 to 0.2 percent (Buesch and Damjanac, 2004). 7) These strain limits determined from geologic relations and rock mechanics modeling are used to determine Peak Ground Velocity (PGV) values that range from about 150 to 450 cm/sec (King and others, 2004). This correlation and linkage of geologic petrogenetic relations for development of features that formed very early in the history of the Topopah Spring Tuff with the types of damage to these features predicted by rock mechanics modeling, and then the incorporation of these limits into the ground motion, represents an integrated approach to assessing the limits on ground motions at Yucca Mountain for the past 12.8 million years.

Acknowledgements

The Detailed Line Survey data in the ECRB cross drift were collected by the Bureau of Reclamation (BOR) and summarized in Mongano and others (1999), and the lithophysal data collected in the cross drift was a collaborative effort by BOR personnel and David Buesch. George Eatman, Jeannie Higgins, and Sheldon Johnson (all of the BOR) assisted in re-examination of previous data and collection of new data that are summarized herein. The data and interpretations summarized herein are based on contributions by Buesch to reports developed for the Yucca Mountain Project (YMP) including the Drift Degradation Analysis (ANL-EBS-000027 Rev 03, 2004), Subsurface Geotechnical Parameters Report (800-K0C-WIS0-00400-000-00A, 2003), and a soon to be completed report Peak Ground Velocities for Seismic Events at Yucca Mountain, Nevada (ANL-MGR-GS-000004 REV 00A, 2004). For the near term, these YMP reports are internal documents; however, they are anticipated to be available on the Office of Civilian Radioactive Waste Management (OCRWM) website (www.ocrwm.doe.gov) or copies can be requested through the Freedom of Information Act.

Petrogenetic sequence of features related to cooling of the Topopah Spring Tuff

In the repository area, the Topopah Spring Tuff is as much as 360-m thick, and greater than 90 percent of the thickness is densely welded, and crystallized ignimbrite (Buesch others, 1999). There are minor variations in the amounts and sizes of lithic and pumice clasts throughout the deposit, but no significant changes occur as evidence for a large hiatus in deposition; therefore, the ignimbrite appears to be deposited by rapid aggradation from a single climactic eruption and pyroclastic flow. Welding of the ignimbrite

probably began during or shortly after deposition, and the rapid aggradation and development of densely welded tuff trapped much of the vapor that initially was interstitial to the vitroclastic grain. The redistribution of the vapor phase during welding resulted in some vapor escaping from the deposit; however, much of the vapor accumulated locally to form lithophysal cavities (Figure 1). Numerical models of compaction and welding in ignimbrites indicate that most of these processes occur in the first few years after deposition (Riehle and others, 1995). Adjacent to the lithophysal cavity walls is an area (volume) referred to as a "rim" that consists of 1) slightly coarser grained and more porous intergrowths of feldspar and SiO2 polymorphs (typically cristobalite or quartz) compared to the surrounding matrix-groundmass, and 2) spherulitic forms of feldspar in the rims. The light gray rims appear to have formed by crystallization of glass in the presence of vapor, but not from the vapor. Likewise, the crystallization of a thin border and surrounding reddish grey matrix-groundmass also appear to have formed from crystallization in the presence of (but lesser interaction with) the outwardly diffusing vapor phase. Crystallization of the glass to form the reddish brown matrix-groundmass is in the absence of the vapor phase. The last feature in lithophysae to develop is the vapor-phase mineral lining (mostly tridymite) that was deposited from the vapor phase during cooling of the rock and vapor. This spatial and temporal development of features (rim, border, reddish grey matrix-groundmass, and vapor-phase mineral lining) also occurs along fractures (Figures 1 and 2).

These relations of spatial and temporal features indicate that the (1) rim, border, and reddish grey matrix-groundmass formed early during cooling of the deposit when the host rock was glass, (2) vapor-phase mineral lining typically formed during late-stage cooling, but actually could develop whenever the vapor became supersaturated in the components that form the vapor-phase minerals, and (3) fractures without rims, borders, or adjacent reddish grey matrix-groundmass and with vapor-phase mineral linings formed during cooling, but after the rock had already crystallized to the matrix-groundmass. It is important to note that some late-stage cooling fractures can form without having vapor-phase mineral coatings simply because once the fracture formed, the geometric relations of the fracture can preclude it from being exposed to the vapor phase. The amount of time needed for a thick, large-volume ignimbrite to cool is poorly constrained; however, it might take several tens of years to perhaps a few hundred years after deposition, but about 100 years after deposition is probably a reasonable period of time. This estimate is based on (1) petrogenetic relations and processes, (2) extrapolations of numerical modeling of welding in ignimbrites (Riehle and others, 1995), and (3) analogy with the Valley of Ten Thousand Smokes in Alaska. The 1912 eruption of the Alaskan Novarupta volcano resulted in pyroclastic flow deposits that might be as great as 200-m thick and formed the Valley of Ten Thousand Smokes (Brantley, 1994); however, the "ten thousand smokes" in the ignimbrite sheet mostly died out by 1930 (Wood and Kienle, 1990).

On the basis of these crystallization and mineralization features, and others such as tubular features and geometric relations, "cooling" fractures are categorized as Type 1 and Type 2 (Buesch and others, 1999), or 1s and 2s, respectively, where fractures are shorter than 1 meter. Fractures that have no cooling related features are categorized as "indeterminate" and could have formed at any time after the rock cooled to ambient paleogeomorphic surface temperatures (these are categorized as Type 3); however, some "indeterminate" fractures can be late-stage cooling fractures that simply do not have the vapor-phase mineralization to identify them as such. To resolve "intermediate" fractures into Type 2 and Type 3 categories, other geometric relations need to be evaluated such as orientation (i.e., strike and dip), trace length, surface morphologic relations (i.e., roughness and planarity on various length scales), and possibly termination characteristics.

Fractures in slabs of core and in the ECRB cross drift

Fractures in 115, spatially distributed core samples from the crystallized Topopah Spring Tuff collected from surface- and tunnel-based boreholes of various sizes were mapped and categorized using 10 characteristics that, in the end, can be simplified into "Cooling" or "Indeterminate" fractures. Core samples are from 10 different lithostratigraphic zones and subzones; however, most are from the upper lithophysal and lower lithophysal zones. Samples from the small-diameter "Thermal Conductivity" (ThermK) boreholes in the upper and lower lithophysal zones are identified as Tptpul*TK and Tptpll*TK, respectively. Map categories were based on how well developed are the crystallization and mineralization features, or the absence of these features, and 2022 fractures were mapped. A ratio of cooling to indeterminate fractures for each sample (i.e., the C/I Ratio) indicates which process dominated the

formation of fractures in the sample. For all lithostratigraphic units (especially those with 5 or more samples), cooling fractures typically are more abundant than indeterminate fractures (Figure 3). The fractures in slabs are categorized into Type 1s, Type 2s, and Indeterminate, but because many fractures have poorly developed rims or borders, a category of "Type 1s+" was (Figure 4). Because of the poor development of features identified with the Type 1s+ fractures, these fractures are transitional from Type 1 to 2, and with the detailed scale of examination in this slab study, many of the Type 1s+ fractures might not have been identified in previous studies. Conclusions from the fractures in slab data include (1) about 70 percent of the fractures are cooling and 30 percent are indeterminate, (2) there are more shorter (less than 1 cm long) fractures per cm^2 of sample in most lithostratigraphic units (especially the lower lithophysal and lower nonlithophysal zones) than fractures that are longer than 1 cm, (3) the largest amount of fractures (and especially cooling fractures) occur in the lower lithophysal zone, and (4) evidence of shear or mechanical fragmentation of a fracture is extremely rare.

A total of 1810 discontinuities (fractures, shears, and faults) were documented in the ECRB cross drift using Detailed Line Survey methods and 21 types of data were collected on all fractures with trace lengths greater than 1 m. Re-examination of the types of material that fills (or partially fills) the fractures (i.e., vapor-phase mineral linings), and characteristic cooling features such as tubular structures, rims, and geometric relations that categorize discontinuities as vapor-phase partings or cooling joints indicates about 71 percent of the fractures are "Cooling" fractures (Types 1, 1+, and 2) and 29 percent are "Indeterminate" fractures (Figure 4). As with the slab study, Type 1+ are transitional from Type 1 to 2. In the cross drift, there are 34 faults or fault zones and 111 shears (i.e., discontinuities with less than 10 cm of slip separation across the feature). Other than the fault and damage zone associated with the 260 m of dip-slip separation on the Solitario Canyon fault (Figure 5), only three faults (the Sundance fault near 11+36, and two "not named" faults at 22+36 and 26+57) have dip-slip separations of greater than 5 m (the diameter of the tunnel), and all other faults have separations of between 0.1 to 2 m (Mongano and others, 1999). Additionally, there are 25 faults and fault zones filled with "fault rubble" or "fault gouge", and 293 discontinuities filled (or partially filled) with "broken or crushed rock or sand" and "breccia" (Figure 5). All shears are filled (or partially filled) with "broken or crushed rock or sand" (Br) or "breccia" (Bx, which is the same as Br, but slightly more lithified), and faults are filled with Br, Bx, fault rubble (Fr), or fault gouge (Fg). This relation of "broken or crushed rock or sand" or "breccia" to shears (and faults) and fractures indicates that approximately 50 percent of discontinuities are filled with broken rock or sand, but they do not have any documented separation across the feature (Figure 5). Additionally, many of the discontinuities with broken rock or sand are also associated with vapor-phase mineral linings (about in the same proportion as fractures without the broken rock or sand). The minimum separation documented on a shear is 1 cm; however, the inference is that some of the fractures simply dilated during cooling (i.e., thermal contraction) or minor extension of the block as a result of tilting along the block bounding faults. Furthermore, the broken rock or sand was apparently deposited into these crevasses because shearing or mechanical degradation of the wall rock does not appear to have been the mechanism to form the broken material. These structural and lithostratigraphic relations from the cross drift indicate that the majority of fractures formed during cooling, some fractures were dilated during cooling (Type 1 or 2) or afterward during minor extension of the structural block associated with faulting and tilting (Type 3), a few "dilated and filled" fractures were sheared, and a very few shears were activated enough to form faults.

Shapes of lithophysae

Lithophysal cavities form as part of the welding process in rocks that are able to viscously deform (i.e., are glass) and have become densely welded. Unlike features such as pumice and shards that collapse during welded, lithophysae inflate to form a variety of shapes. Four main shapes of lithophysal cavities have been documented in the Topopah Spring Tuff (and other tuffs) including (1) simple, (2) cuspate, (3) merged, and (4) expansion-crack lithophysae (Figure 6). All these shapes can vary in aspect ratio (in a 2-dimensional cross section it is the longest axis divided by the shortest axis), and the ratios can range from about 20 to 1 (or sometimes reported as 20:1 to 1:1) where 1 represents a circle. "Simple" shapes are ovoid (possibly even lens- or disk-shaped) (Figure 6A). Typically, there are small (a few millimeters wide and deep) expansion cracks that formed as the rim crystallized, but as the gas pressure continued to increase, the rim fractured during inflation and the "plates" of the cavity walls moved apart (Figure 6B). Where walls between two or more lithophysae were breached during the inflation of the cavities, merged lithophysae were formed (Figure 6C). Formation of some lithophysae were controlled by propagation of early-formed

expansion cracks to form irregular or "star burst" shapes; hence the name "expansion-crack" lithophysae (Figure 6D). "Cuspate" lithophysae are typically fairly simple in shape, although one or more parts of the cavity wall merge into fractures such that the cavity appears to have partially collapsed (possibly during release of the vapor along the fractures). Some cuspate lithophysae might be part of larger expansion-crack lithophysae; however, the exposure is such that the complete shape of the lithophysae can not be identified. These shapes of cavities are all consistent with processes that could have been (were) active during the early formation of the lithophysae.

During mapping between 2001 and 2004, the four main shapes of lithophysal cavities (simple, cuspate, merged, and expansion-crack lithophysae) have been documented for 1434 lithophysae in the Topopah Spring Tuff along the cross drift (Figure 7). Mapping and documentation of lithophysae included use of Panel Maps and Panel Photographs (maps drawn on photographs of cleaned tunnel walls), two types of linear traverses, and lithophysae-specific inventories (i.e., point data). Panel Maps are 1x3-m-sized areas in which all lithostratigraphic features are mapped, including lithophysal cavities, and Panel Photographs are 2x7-m-sized areas in which only lithophysae larger than 20 cm in diameter were photographically identified as to shape of the lithophysal cavities. In the Panel Photographs, 34 lithophysae are "backfilled" with "muck" from the tunnel boring machine (i.e., they were not completely cleaned out during washing of the wall), so specific shapes could not be clearly identified; however, none appeared to be collapsed. Although the lithophysae data were largely collected for other mapping efforts, the compilation of available data indicates that none of the lithophysal cavities exhibited any evidence for damage or collapse structures. Additionally, only 18 lithophysae are intercepted (partially or transected) by fractures, and only 5 are transected by shears. Modeling of lithophysal and nonlithophysal tuff using the rock mechanics "Universal Distinct Element Code" (UDEC) with various seismic waveform and particle velocity data sets indicates that some sets result in extensive damage to the rock mass. The lack (or rarity) of damage to lithophysae in the cross drift indicates that the rock mass probably has not been subjected to the larger values of ground motions (Buesch and Damjanic, 2004).

Relations of fractures and lithophysae

The relations of fractures and lithophysal cavities were not explicitly mapped during the lithophysal studies between 2001 and 2004; however, rock mechanics modeling using the "Particle Flow Code" (PFC) indicates that when rocks are strained to the point of failure, a characteristic inter-lithophysae fracture pattern develops (Figure 8, Buesch and Damjanic, 2004). The PFC model is a 1x1-m area where lithophysae are represented as voids in the "rock material", and some model runs used "stenciled" shapes of lithophysal cavities from Panel Maps (Figure 8). "Stenciled", unconfined compression test, PFC model runs such as those in Panel Map "1624" indicate (1) peak strain at failure of 0.17 to 0.30 percent with (2) micro-fractures in blue formed at pre-peak-strength failure, (3) micro-fractures in red formed at post peak-strength failure, and (4) development of inter-lithophysal fracture patterns. Using photographic interpretation methods, a total of 300 fractures were mapped on the photograph used for the Panel Map at 1624 on the right wall of the cross drift, and although there are a few fractures that intersect lithophysal cavities, the inter-lithophysal fracture pattern did not develop in this rock (Figure 8). A total of 38 Panel Map and Panel Photographs were photographically reviewed for the inter-lithophysal fracture pattern, and again, although there are a few fractures that intersect lithophysal cavities, the inter-lithophysal fracture pattern did not develop in these rocks.

Summary of geologic and rock mechanics limits on ground motion

The petrogenetic sequence of lithostratigraphic feature development in the densely welded and crystallized Topopah Spring Tuff provides textural and mineralogical evidence that the lithostratigraphic features and most of the fractures formed in a relatively short period of time (possibly 100 years) after deposition of the tuff. Rock mechanics models such as UDEC and PFC provide quantitative values of rock strengths for the failure of the rocks, and "predictions" of features such as damaged (collapsed) or inter-lithophysal fracture patterns that would develop where rocks are statically or dynamically strained beyond their failure strength. The overall lack of damage to "cooling" related features such as lithophysae and most fractures is consistent with the rock mass of the Topopah Spring Tuff having never been strained beyond the static or dynamic failure strength since deposition 12.8 million years ago. However, fracture-fill materials and geometric relations of discontinuities in the cross drift indicate that strain has been localized along a relatively few faults and distributed along 141 minor faults and shears.

References

Brantley, S.R. 1994. Volcanoes of the United States. VOLCUS1994: U.S. Geological Survey, Information Services, 12 p.

Buesch, D.C., and Damjanac, Branko, 2004, Geologic and rock mechanics limits on maximum potential strain in the 12.8-M.Y. history of the Topopah Spring Tuff at Yucca Mountain, Nevada: Geological Society of America, Boulder, Colorado, Annual Meeting Abstracts with Programs, v. 36, no. 5, p. 33.

Buesch, D.C., Beason, S.C., and Spengler, R.W., 1999, Relations among welding, vapor-phase activity, crystallization, and fractures in the Tiva Canyon and Topopah Spring Tuffs at Yucca Mountain, Nevada: Geological Society of America Abstracts with Programs, v. 31, p. A476-A477.

Buesch, D.C., and Spengler, R.W., 1998, Character of the middle nonlithophysal zone of the Topopah Spring Tuff at Yucca Mountain: *in* International High-Level Radioactive Waste Management Conference, American Nuclear Society, Le Grange Park, Illinois, p. 16-23.

Buesch, D.C., Spengler, R.W., Moyer, T.C., and Geslin, J.K., 1996, Proposed stratigraphic nomenclature and macroscopic identification of lithostratigraphic units of the Paintbrush Group exposed at Yucca Mountain, Nevada: U. S. Geological Survey Open-File Report 94-469, 47 p.

Flint, L.E., 1998, Characterization of Hydrogeologic Units Using Matrix Properties, Yucca Mountain, Nevada: U.S. Geological Survey Water-Resources Investigations Report 97-4243, 64 p.

King, J.L, Coppersmith, K.J, and Quittmeyer, R.C., 2004, Bounding peak ground velocities for seismic events at Yucca Mountain, Nevada: Geological Society of America, Boulder, Colorado, Annual Meeting Abstracts with Programs, v. 36, no. 5, p. 33.

Mongano, G.S.; Singleton, W.L.; Moyer, T.C.; Beason, S.C.; Eatman, G.L.W.; Albin, A.L.; and Lung, R.C. 1999, Geology of the ECRB Cross Drift - Exploratory Studies Facility, Yucca Mountain Project, Yucca Mountain, Nevada: Bureau of Reclamation and U.S. Geological Survey accessed April 16, 2004 at http://www.ocrwm.doe.gov/technical/doclist.

Munsell Color Company, 2000, "Munsell Soil Color Charts, 2000 Revised Edition" GretagMacbeth, New Windsor, New York., 11 p., 20 plates.

Otto, S.J., and Buesch, D.C. 2003, Porosity, bulk density, and rock-particle density of lithostratigraphic components in lithophysal rocks of the Topopah Spring Tuff at Yucca Mountain, Nevada: Geological Society of America Abstracts with Programs, v. 35, no. 6, p. 434-435.

Riehle, J.R.; Miller, T.F.; and Bailey, R.A. 1995, Cooling, Degassing and Compaction of Rhyolitic Ash Flow Tuffs: A Computational Model: Bulletin of Volcanology, v. 57, no. 5, p. 319-336.

Wood, C.A. and Kienle, J., eds. 1990. "Volcanoes of North America, United States and Canada", Cambridge University Press, Cambridge, England, p. 70.

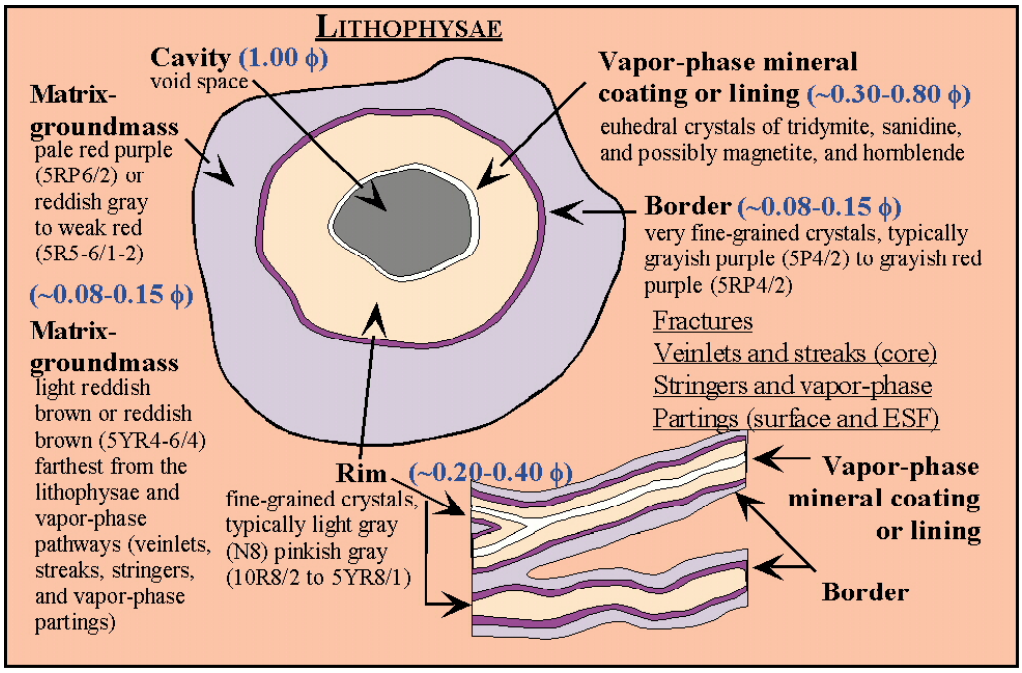

Figure 1. Welding, crystallization, and mineralization features related to lithophysae and fractures in densely welded and crystallized Topopah Spring Tuff. Porosity values for the matrix-groundmass are from Otto and Buesch (2003), approximated from Flint (1998), and Buesch (2003, not published). Values for rims are from Otto and Buesch (2003), and the values for borders and vapor phase mineral coatings are estimates by Buesch (2003, not published). Nomenclature and symbols of colors (e.g., pale red purple is 5RP6/2) are based on comparisons with the Munsell Soil Color Chart (Munsell Color Company 1994).

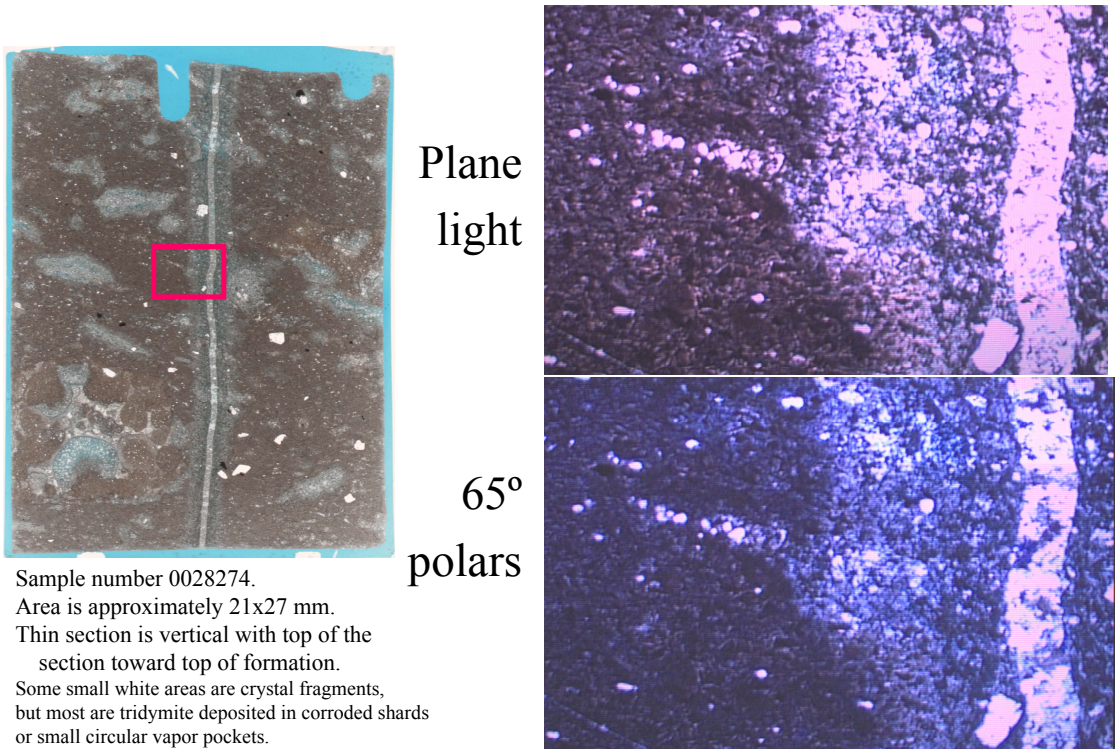

Figure 2. Thin section and photomicrographs of densely welded and crystallized Topopah Spring Tuff from the middle nonlithophysal zone (Tptpmn) in borehole USW NRG-6 at a depth of 730 ft. The rim and vapor-phase mineral lining are identifiable in the full thin section and in the close up views.

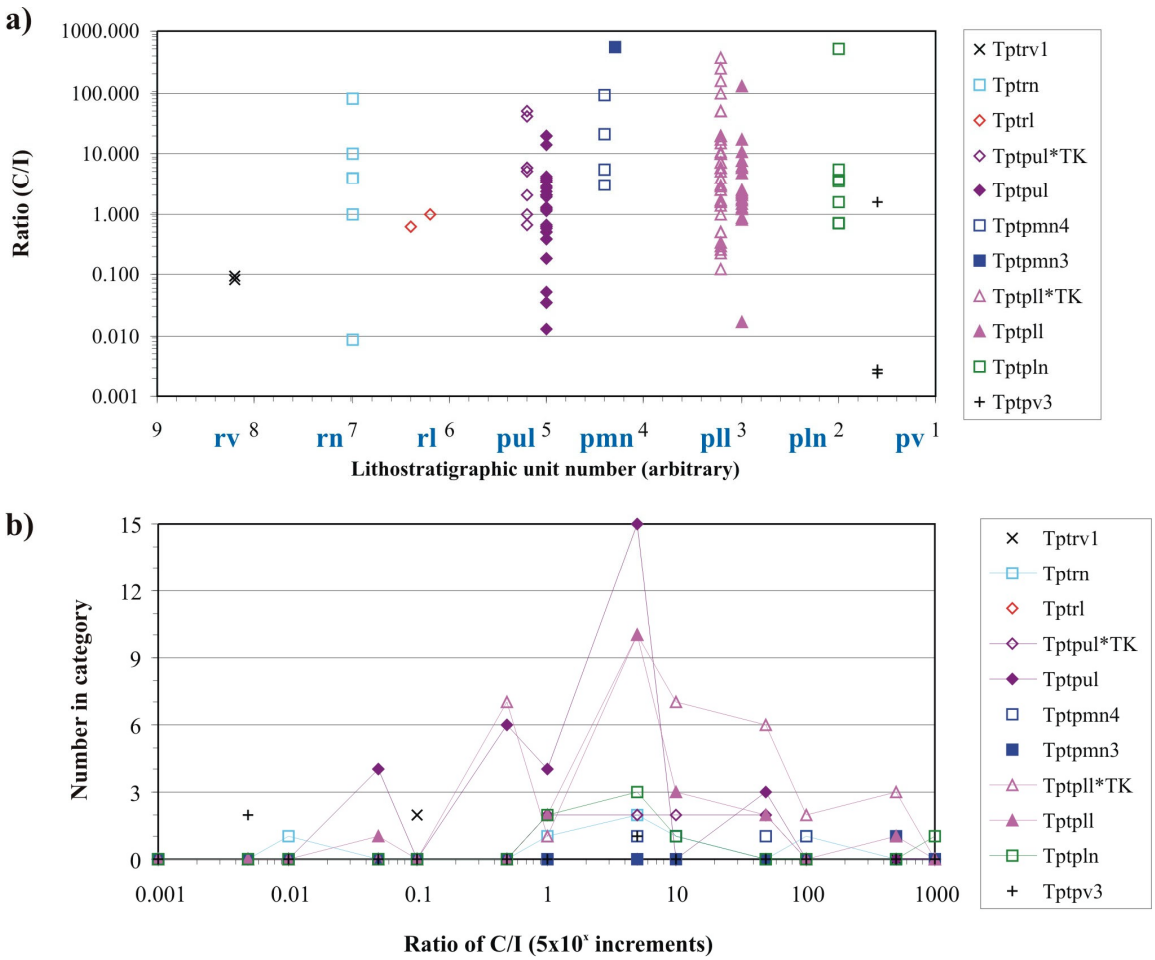

Figure 3. "Cooling to Indeterminate Ratio" (C/I Ratio) of fractures by lithostratigraphic zone or subzone in the densely welded and crystallized Topopah Spring Tuff. A) C/I Ratios of individual samples plotted by lithostratigraphic zone or subzone. B) The number of C/I Ratio values in $5x10^x$ increments plotted by lithostratigraphic zone or subzone. Lines are only plotted for units with 5 or more samples

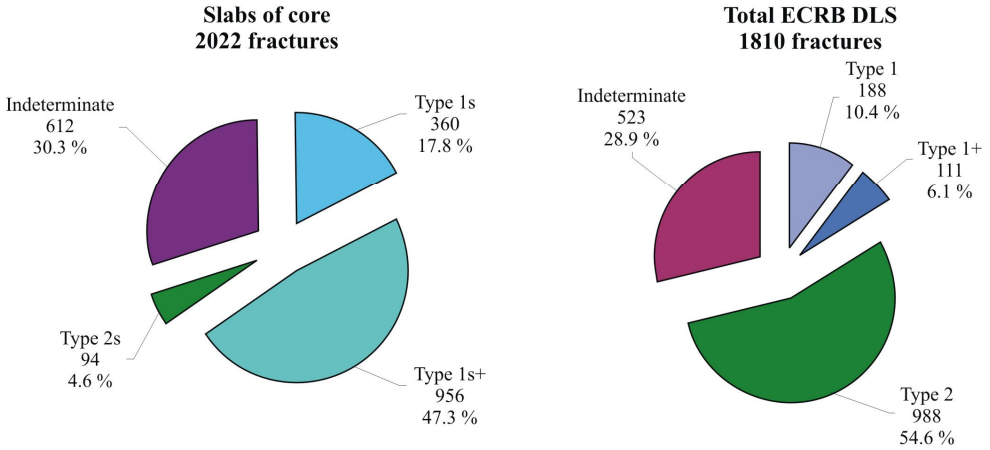

Figure 4. "Cooling" fractures (Type 1, 1+, and 2) and "Indeterminate" fractures in slabs of core and ECRB DLS data. In the DLS data, plots of trace length and orientation (stereo plots) indicate vary similar geometric relations of cooling and indeterminate fractures.

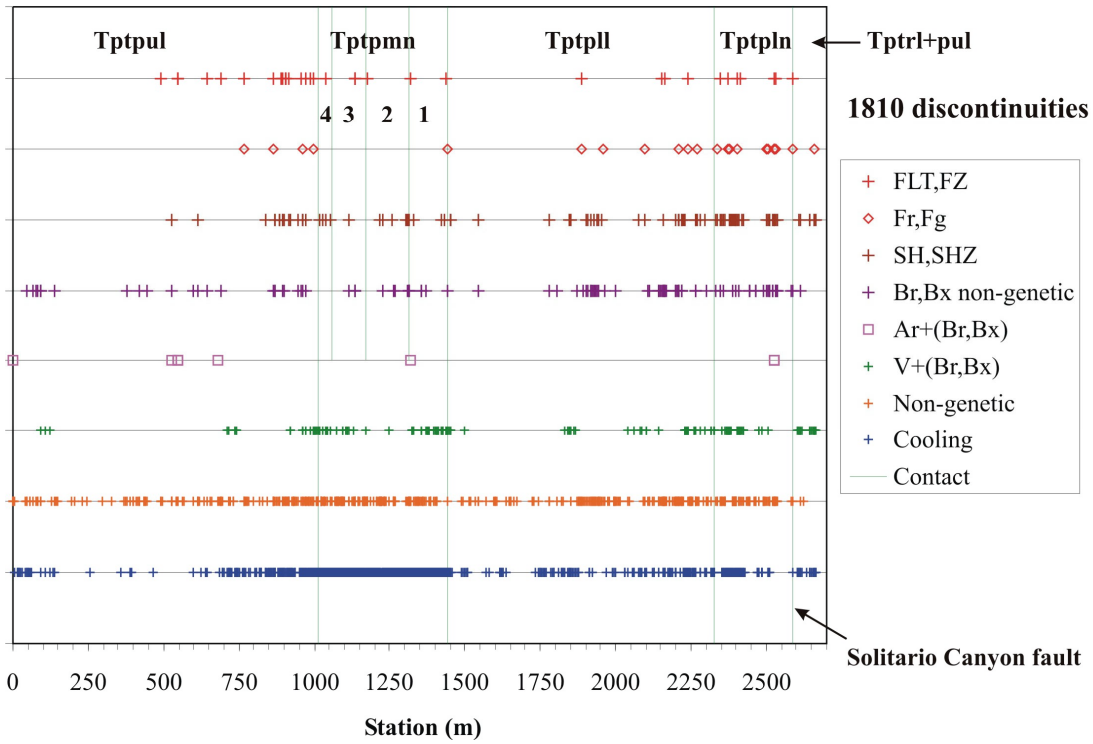

Figure 5. Distribution of discontinuities along the ECRB cross drift identified as "Cooling", "Non-genetic" (or indeterminate), those filled with "broken or brecciated rock, or sand" (Br or Bx), shears and shear zones (SH and SHZ), faults and fault zones (FLT and FZ), and fault breccia or fault gouge (Fr or Fg). Fracture-fill conditions with "broken or brecciated rock, or sand" that include clay [Ar+(Br,Bx)], and vapor-phase minerals [V+(Br,Bx)].

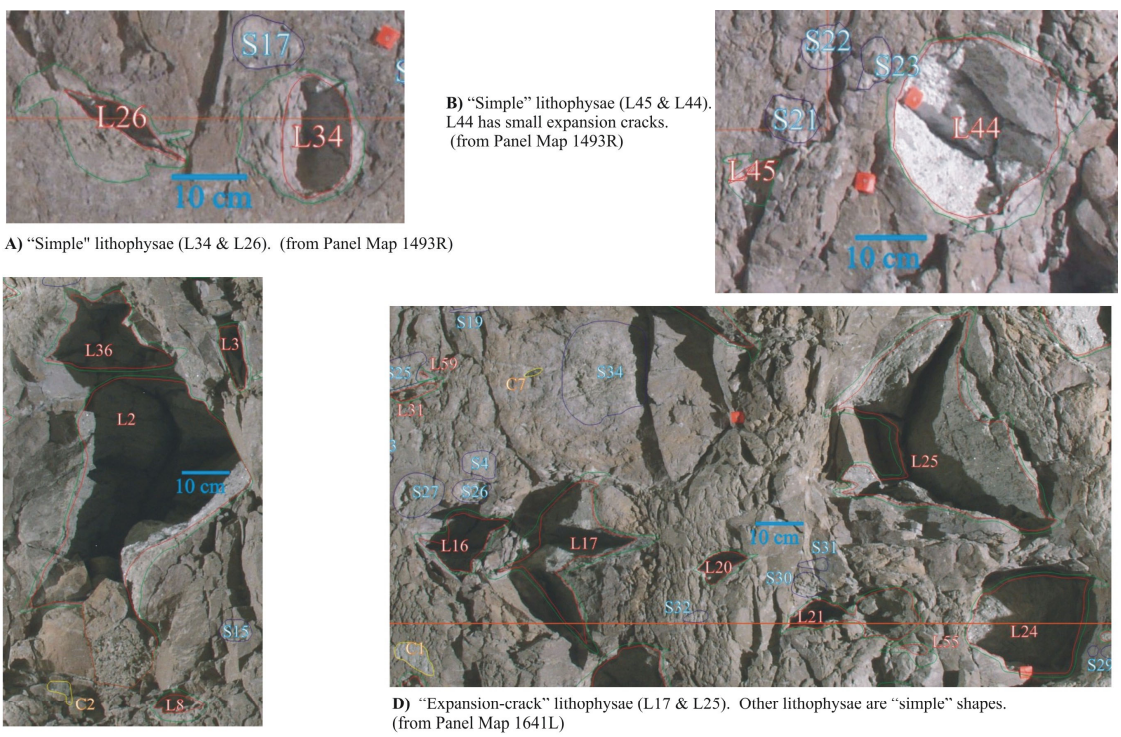

Figure 6. Shapes of lithophysae in the densely welded and crystallized Topopah Spring Tuff.

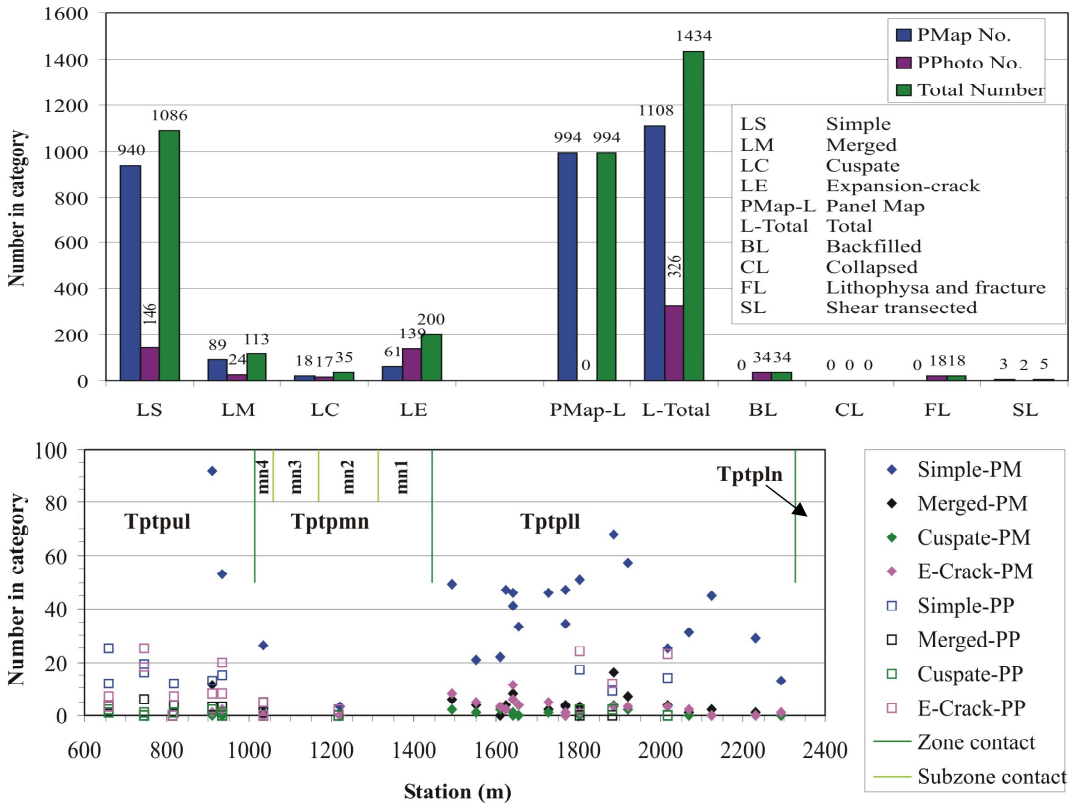

Figure 7. Summary of shapes of lithophysae in the Topopah Spring Tuff exposed in the ECRB cross drift and cataloged in Panel Maps (PM) and Panel Photographs (PP).

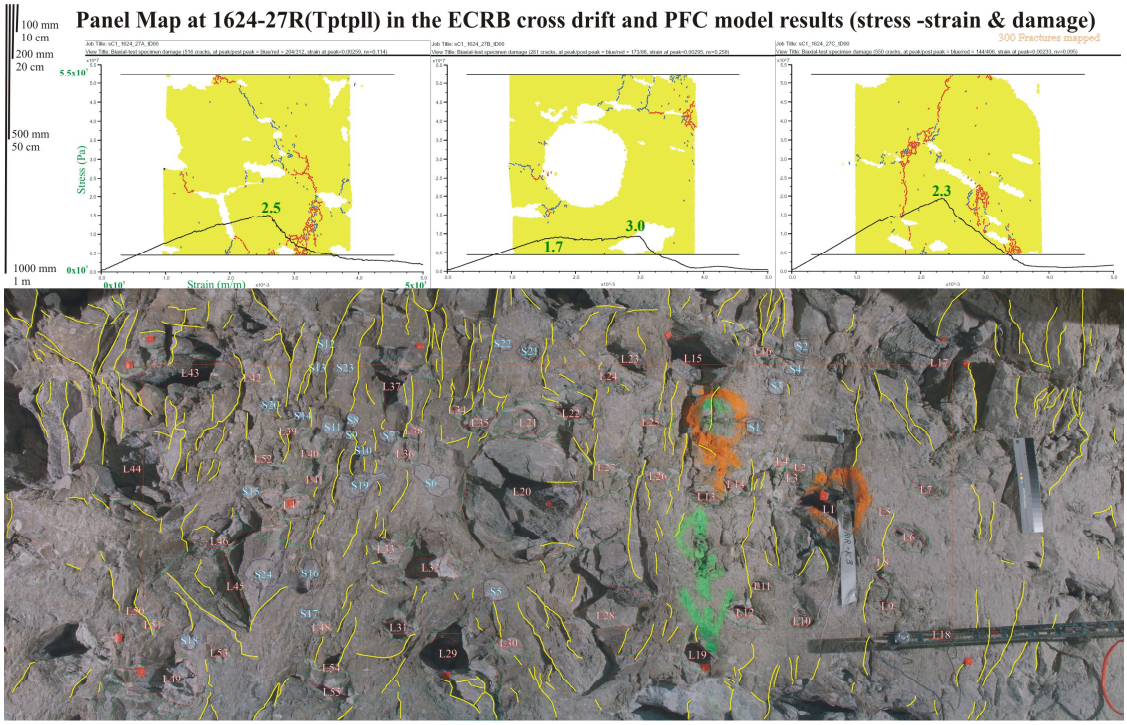

Figure 8. Panel Map location 1624 to 1627 on the right wall of the ECRB cross drift with overlays of 300 photographically interpreted fracture traces. The inset diagrams are of the PFC results from the 1x1-m stenciled models and the associated stress-strain relations.